



Supplement of

Distinguishing the impacts of natural and anthropogenic aerosols on global gross primary productivity through diffuse fertilization effect

Hao Zhou et al.

Correspondence to: Xu Yue (yuexu@nuist.edu.cn)

The copyright of individual parts of the supplement might differ from the article licence.

Table S1 Information of CEDS inventory

Source sector	Emission species	Date sources ^a
Fuel combustion	NO _x , NMVOC _s , CO, CH ₄ BC, OC SO ₂ NH ₃ CO ₂	GAINS energy use and emissions SPEW energy use and emissions GAINS sulfur content and ash retention (Europe), and local emission data US NEI energy use and emissions CDIAC and additional data sources
Fugitive petroleum and gas	ALL	EDGAR emissions and ECLIPSE V5a
Cement	CO ₂	CDIAC
Agriculture	CH ₄ Other	FAOSTAT and EDGAR EDGAR
Waste combustion	ALL	Estimation with methods from references
Waste water treatment	NH ₃	CEDS estimate of NH ₃ from human waste
Other non-combustion	SO ₂ ALL	EDGAR and other data sources EDGAR emissions

^a More detailed information can be found at Hoesly *et al.* (2018)

Table S2 Summary of simulations for aerosol diffuse fertilization effects

Simulations	Models	Input	Aerosol	Cloud	Output
GC_ALL	GEOS-Chem	All emissions	All aerosols	Obs.	Monthly 3-D aerosol concentrations
GC_NAT		All without anth. emissions	Natural aerosols		
CRM_ALL_CLD	CRM	Aerosols from GC_ALL	All aerosols	Obs.	Hourly direct and diffuse PAR at surface
CRM_NAT_CLD		Aerosols from GC_NAT	Natural aerosols		
CRM_NO_CLD		No aerosol input	NO aerosols		
CRM_ALL_BCCLD		BC from GC_ALL	BC (natural+ anth.)		
CRM_NAT_BCCLD		BC from GC_NAT	BC (natural)		
CRM_ALL_OCCLD		OC from GC_ALL	OC (natural+ anth.)		
CRM_NAT_OCCLD		OC from GC_NAT	OC (natural)		
CRM_ALL_SNCLD		Sulfate/Nitrate from GC_ALL	Sulfate/Nitrate (natural+ anth.)		
CRM_NAT_SNCLD		Sulfate/Nitrate from GC_NAT	Sulfate/Nitrate (natural)		
CRM_NAT_SSCLD		Sea salts from GC_NAT	Sea salt (natural)		
CRM_NAT_DSCLD		Dust from GC_NAT	Dust (natural)		
CRM_ALL_CLR		Aerosols from GC_ALL	All aerosols	None	
CRM_NAT_CLR		Aerosols from GC_NAT	Natural aerosols		
CRM_NO_CLR		No aerosol input	NO aerosols		
CRM_ALL_BCCLR		BC from GC_ALL	BC (natural+ anth.)		
CRM_NAT_BCCLR		BC from GC_NAT	BC (natural)		
CRM_ALL_OCCLR		OC from GC_ALL	OC (natural+ anth.)		
CRM_NAT_OCCLR		OC from GC_NAT	OC (natural)		
CRM_ALL_SNCLR		Sulfate/Nitrate from GC_ALL	Sulfate/Nitrate (natural+ anth.)		
CRM_NAT_SNCLR		Sulfate/Nitrate from GC_NAT	Sulfate/Nitrate (natural)		
CRM_NAT_SSCLR		Sea salts from GC_NAT	Sea salt aerosols (natural)		
CRM_NAT_DSCLR		Dust from GC_NAT	Dust aerosols (natural)		
YIBS_ALL_CLD	YIBs	PAR from CRM_ALL_CLD	All aerosols	Obs.	Monthly GPP
YIBS_NAT_CLD		PAR from CRM_NAT_CLD	Natural aerosols		
YIBS_NO_CLD		PAR from CRM_NO_CLD	NO aerosols		
YIBS_ALL_BCCLD		PAR from CRM_ALL_BCCLD	BC (natural+ anth.)		
YIBS_NAT_BCCLD		PAR from CRM_NAT_BCCLD	BC (natural)		
YIBS_ALL_OCCLD		PAR from CRM_ALL_BCCLD	OC (natural+ anth.)		
YIBS_NAT_OCCLD		PAR from CRM_NAT_OCCLD	OC (natural)		
YIBS_ALL_SNCLD		PAR from CRM_ALL_SNCLD	Sulfate/Nitrate (natural+ anth.)		
YIBS_NAT_SNCLD		PAR from CRM_NAT_SNCLD	Sulfate/Nitrate (natural)		
YIBS_NAT_SSCLD		PAR from CRM_NAT_SSCLD	Sea salt (natural)		
YIBS_NAT_DSCLD		PAR from CRM_NAT_DSCLD	Dust (natural)		
YIBS_ALL_CLR		PAR from CRM_ALL_CLR	All aerosols	None	
YIBS_NAT_CLR		PAR from CRM_NAT_CLR	Natural aerosols		
YIBS_NO_CLR		PAR from CRM_NO_CLR	NO aerosols		
YIBS_ALL_BCCLR		PAR from CRM_ALL_BCCLR	BC (natural+ anth.)		
YIBS_NAT_BCCLR		PAR from CRM_NAT_BCCLR	BC (natural)		

YIBS_ALL_OCCLR		PAR from CRM_ALL_OCCLR	OC (natural+ anth.)		
YIBS_NAT_OCCLR		PAR from CRM_NAT_OCCLR	OC (natural)		
YIBS_ALL_SNCLR		PAR from CRM_ALL_SNCLR	Sulfate/Nitrate (natural+ anth.)		
YIBS_NAT_SNCLR		PAR from CRM_NAT_SNCLR	Sulfate/Nitrate (natural)		
YIBS_NAT_SSCLR		PAR from CRM_NAT_SSCLR	Sea salt aerosols (natural)		
YIBS_NAT_DSCLR		PAR from CRM_NAT_DSCLR	Dust aerosols (natural)		

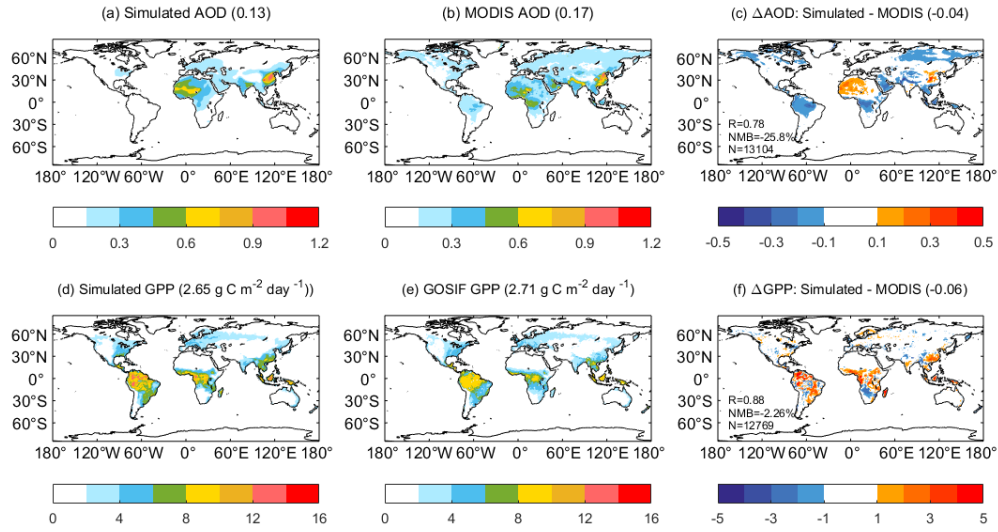


Figure S1 Evaluations of simulated AOD by GEOS-Chem and GPP by YIBs model. Results shown are the annual (a, b) AOD at 550 nm and (d, e) GPP from (a, d) simulations, (b, e) observations and (c, f) their differences during 2001-2014. Simulated AOD is performed with the GEOS-Chem chemical transport model, which is driven with MERRA meteorology and emissions from anthropogenic and natural sources. Observed AOD is retrieved from the Moderate Resolution Imaging Spectroradiometer (MODIS, <https://modis.gsfc.nasa.gov>). Simulated GPP is derived using YIBs vegetation model, which is driven with hourly $1^\circ \times 1^\circ$ meteorological forcings from MERRA-2 reanalyses. Observed GPP is derived from global OCO-2-based SIF product with linear relationships between SIF and GPP (Li & Xiao, 2019). The R, NMB and N are shown in (c) and (f).

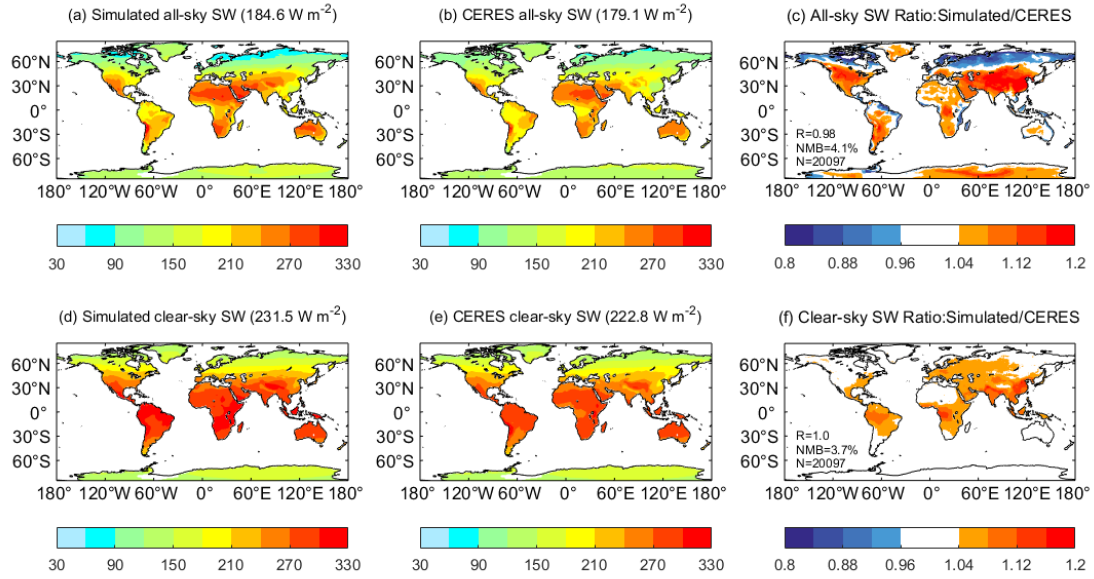


Figure S2 Evaluations of simulated shortwave radiation (SW) by CRM model. Results shown are the annual (a, b) all-sky and (d, e) clear-sky SW from (a, d) simulations, (b, e) observations and (c, f) their ratios during 2001-2014. Simulations are derived using the Column Radiation Model (CRM), which is driven with hourly $1^\circ \times 1^\circ$ meteorological forcings from MERRA-2 and cloud profiles from the SYN1deg product of CERES. Observed SW is adopted from the CERES SYN1deg datasets. The R, NMB and N are shown in (c) and (f).

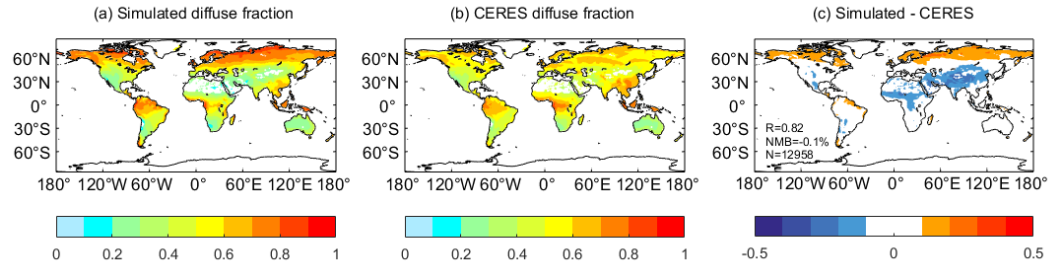


Figure S3 Evaluations of simulated diffuse fraction (DF) by CRM model. Results shown are the annual DF from (a) simulations, (b) observations and (c) their differences over land vegetated grids during 2001-2014. Simulations are performed using the Column Radiation Model (CRM), which is driven with hourly $1^\circ \times 1^\circ$ meteorological forcings from MERRA-2 and cloud profiles from the SYN1deg product of CERES. The R, NMB and N are shown in (c).

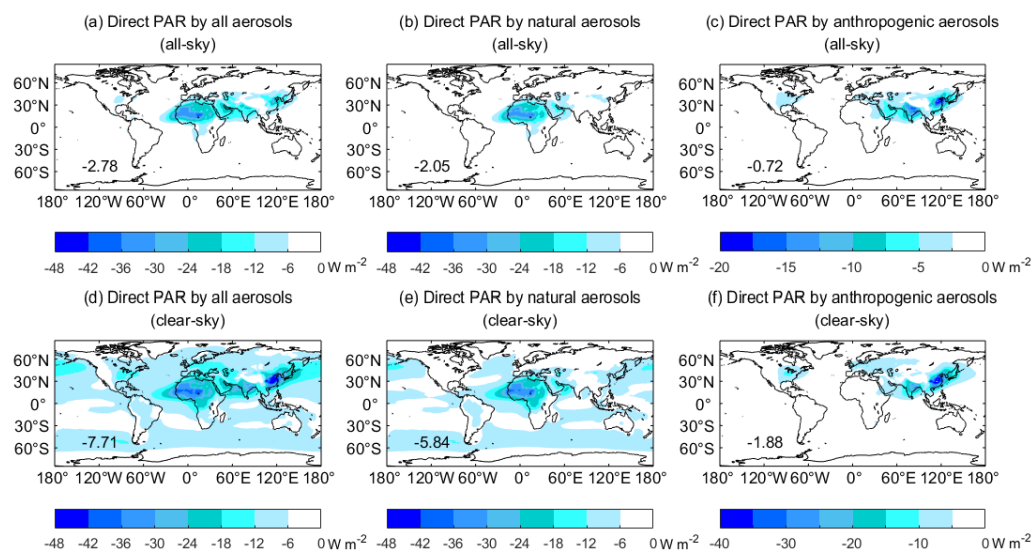


Figure S4 Global direct PAR changes at surface by all, natural and anthropogenic aerosols at (a, b, c) all-sky and (d, e, f) clear-sky conditions. The units are W m^{-2} . The global changes in direct PAR caused by different aerosol sources are shown on corresponding panels. Please notice that the color scales for natural and anthropogenic aerosols are different.

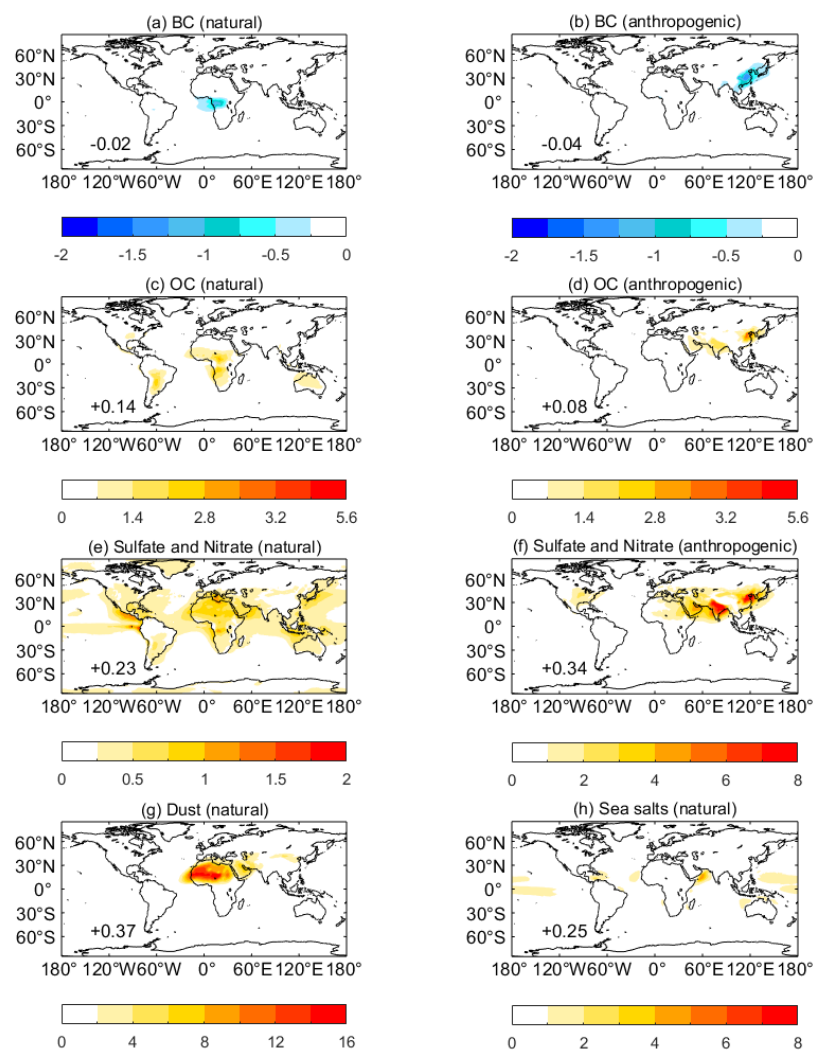


Figure S5 Global diffuse PAR changes by specific natural and anthropogenic aerosols at all skies. The units are W m⁻². The global changes in diffuse PAR caused by individual aerosol species are shown on corresponding panels. Please notice that the color scales for different aerosol species are different.

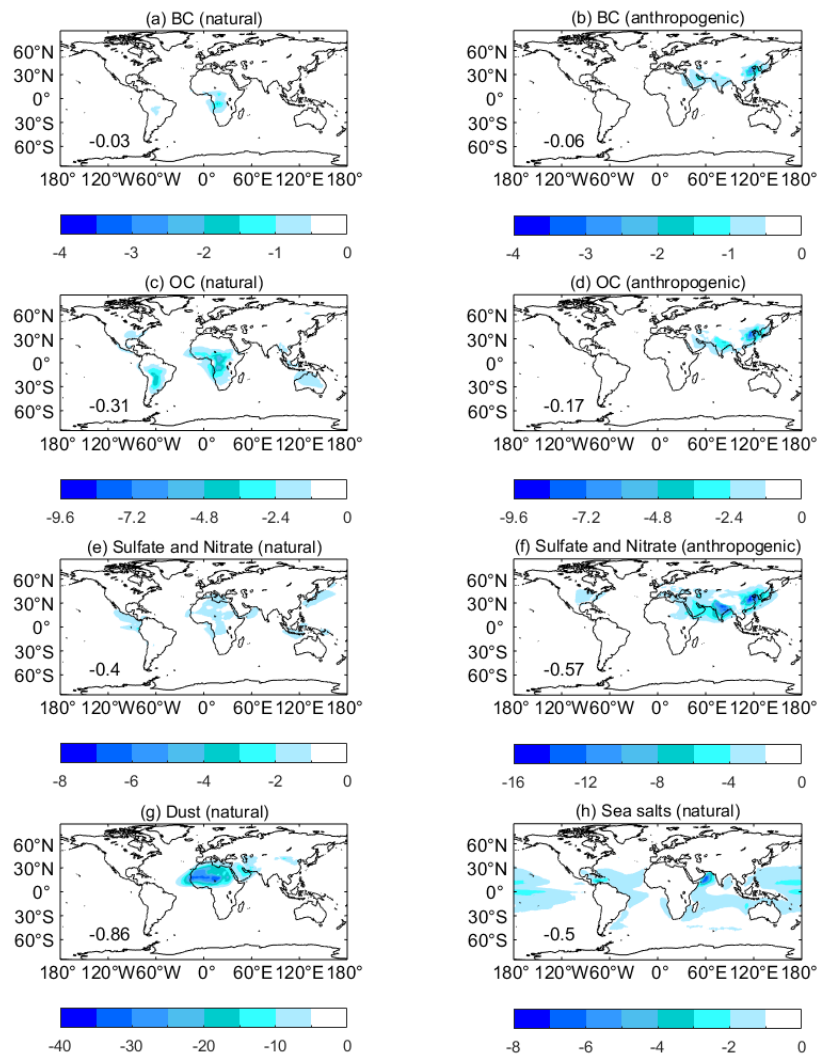


Figure S6 Global direct PAR changes by specific natural and anthropogenic aerosols at all skies. The units are W m^{-2} . The global changes in direct PAR caused by individual aerosol species are shown on corresponding panels. Please notice that the color scales for different aerosol species are different.

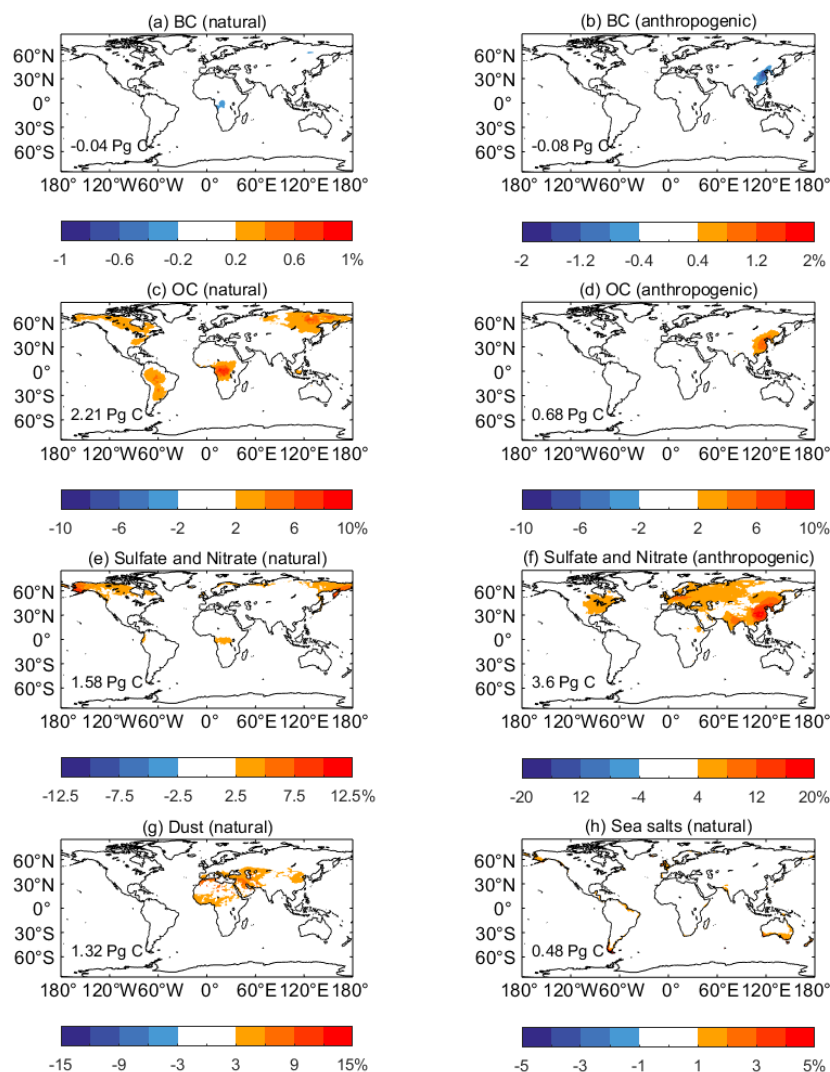


Figure S7 Percentage changes in GPP by specific natural and anthropogenic aerosols at clear skies. The units are %. The global changes in GPP caused by individual aerosol species are shown on corresponding panels. Please notice that the color scales for different aerosol species are different.

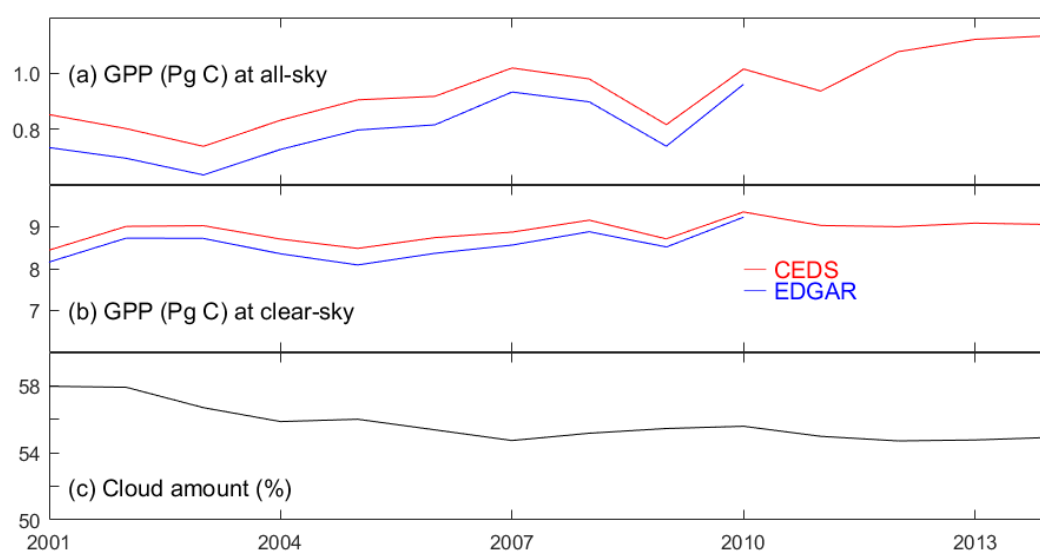


Figure S8 The interannual variations of global GPP changes caused by aerosol DFE at (a) all skies and (b) clear skies, and (c) the simultaneous changes in cloud amount (%) during 2001-2014. The aerosols are simulated using anthropogenic emissions from CEDS (red) and EDGAR (blue).

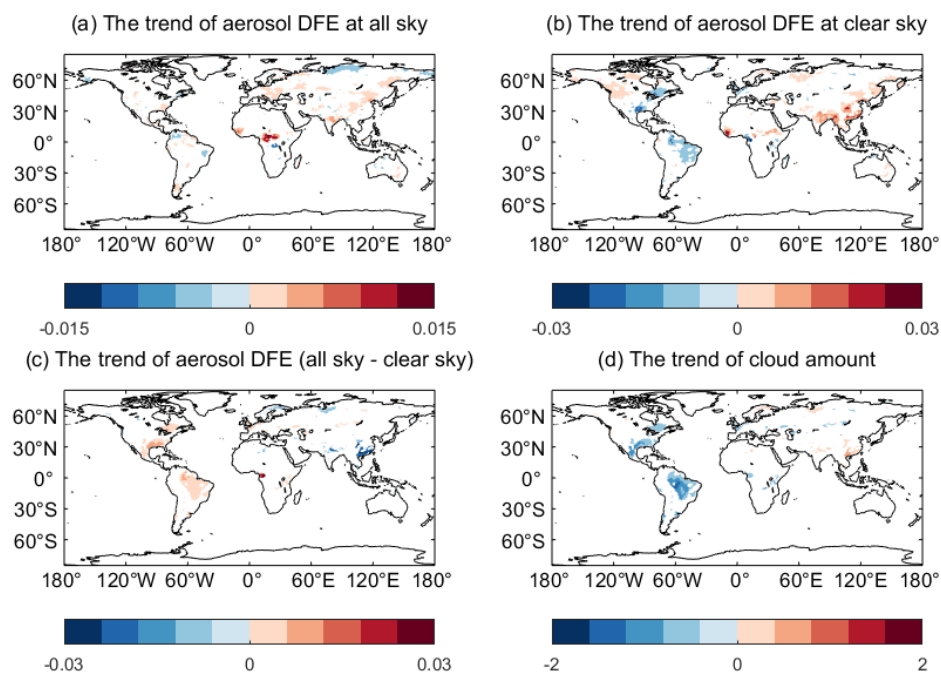


Figure S9 Trends of aerosol DFE ($\text{g C m}^{-2} \text{ day}^{-1} \text{ yr}^{-1}$) at (a) all skies and (b) clear skies. The difference between (a) and (b) is presented in (c), and the trend of cloud amount ($\% \text{ yr}^{-1}$) is shown in (d). Only the significant trends ($p < 0.05$) are presented.

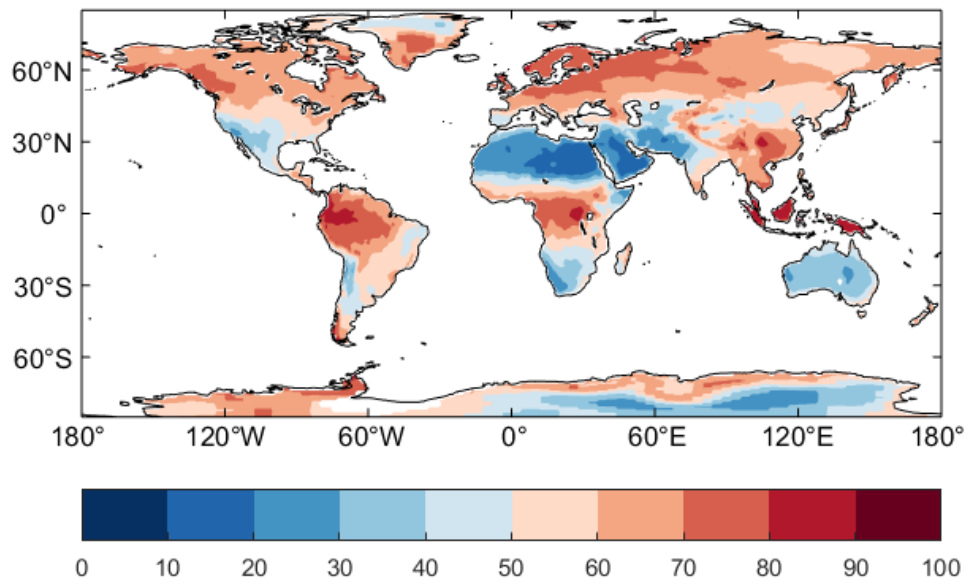


Figure S10 Spatial distribution of global cloud amount. Results shown are annual average cloud fraction (%) from the SYN1deg product of NASA Clouds and the Earth's Radiant Energy System (CERES) during 2001-2014.

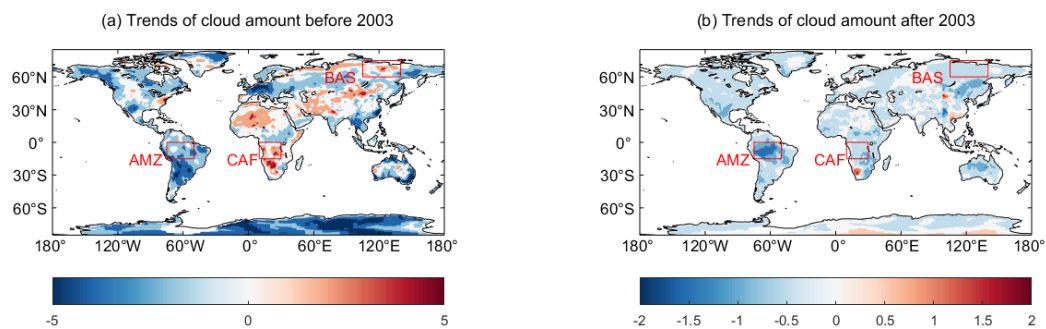


Figure S11 Trends of cloud amount before 2003 (a) and after 2003 (b). The regions marked in map include Amazon (AMZ), central Africa (CAF) and boreal Asia (BAS). The units $\% \text{ yr}^{-1}$.

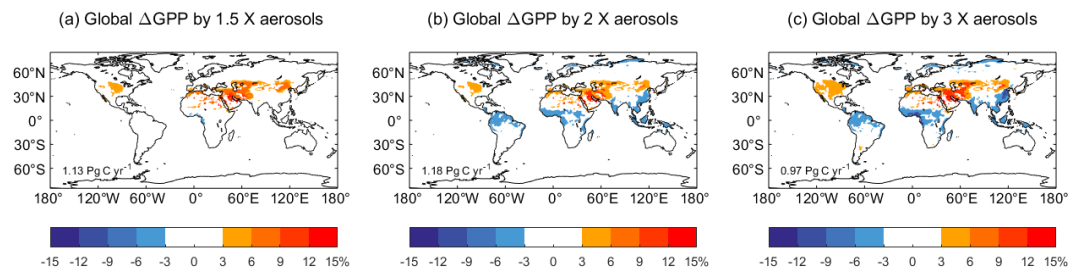


Figure S12 The same as Figure 3a but with 1.5, 2, and 3 times of aerosol concentrations.

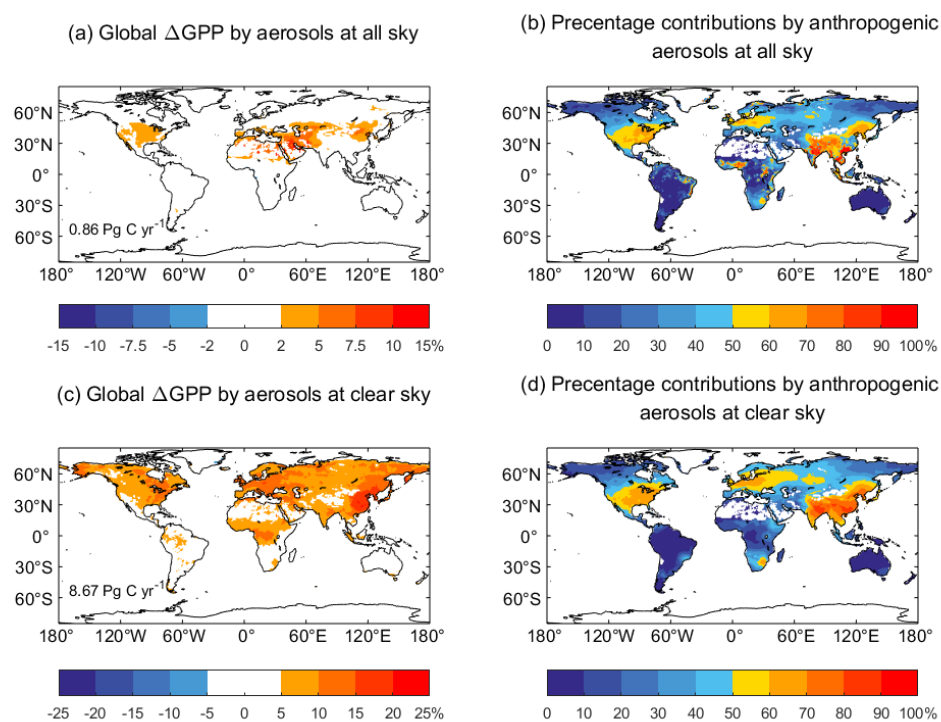


Figure S13 The same as Figure 3 but with anthropogenic emissions from EDGAR.

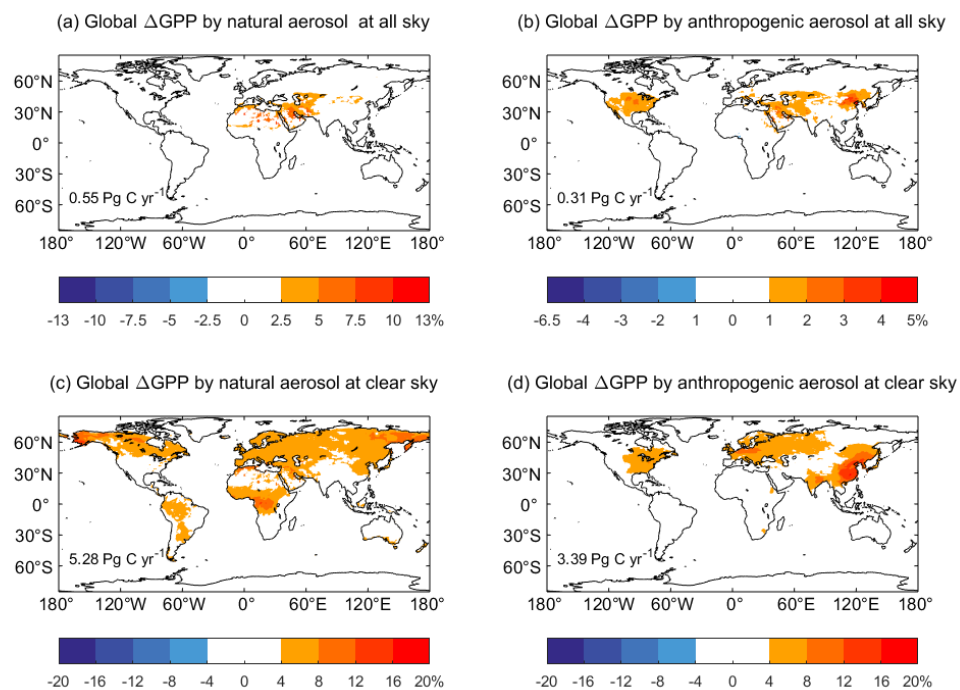


Figure S14 The same as Figure S6 but with anthropogenic emissions from EDGAR.

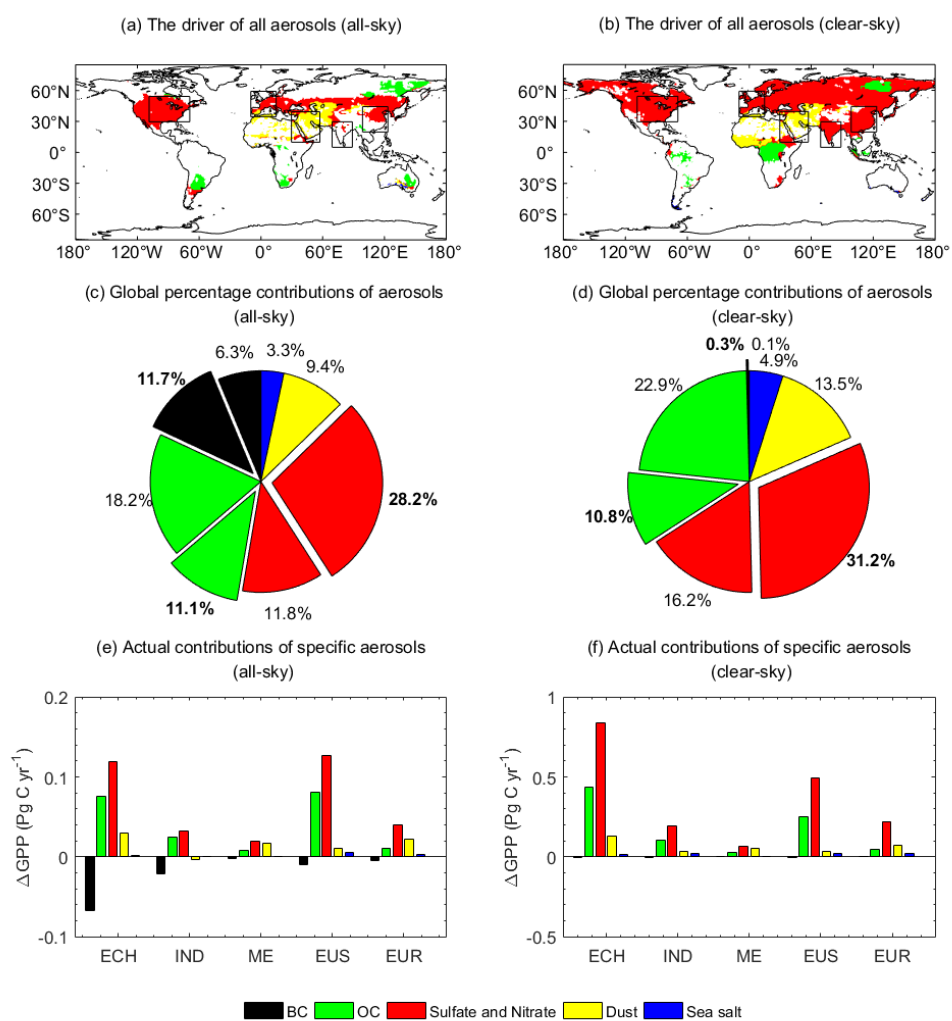


Figure S15 The same as Figure 6 but with anthropogenic emissions from EDGAR.

Reference:

Hoesly RM, Smith SJ, Feng L *et al.* (2018) Historical (1750-2014) anthropogenic emissions of reactive gases and aerosols from the Community Emissions Data System (CEDS). *Geoscientific Model Development*, **11**, 369-408.